Fine Structure of the Pygmy Dipole Resonance in ^{136}Xe

D. Savran,[1,*] M. Fritzsche,[1] J. Hasper,[1] K. Lindenberg,[1] S. Müller,[1] V. Yu. Ponomarev,[1,†] K. Sonnabend,[1] and A. Zilges[2]

[1]*Institut für Kernphysik, TU Darmstadt, Schlossgartenstraße 9, D-64289 Darmstadt, Germany*

[2]*Institut für Kernphysik, Universität zu Köln, Zülpicher Straße 77, D-50937 Köln, Germany*

(Received 21 February 2008; published 11 June 2008)

The photoresponse of the semimagic $N = 82$ nucleus ^{136}Xe was measured up to the neutron separation energy S_n using the (γ, γ') reaction. A concentration of strong dipole excitations is observed well below S_n showing a fragmented resonancelike structure. Microscopic calculations in the quasiparticle phonon model including complex configurations of up to three phonons agree well with the experimental data in the total integrated strength, in the shape and the fragmentation of the resonance, which allows us to draw conclusions on the damping mechanism of the pygmy dipole resonance.

DOI: 10.1103/PhysRevLett.100.232501 PACS numbers: 25.20.Dc, 21.60.Jz, 24.30.Gd, 27.60.+j

Collective excitations are a common phenomenon in many-body physics. Giant resonances are a classical example of collective excitations in atomic nuclei. The theoretical description of the damping of these collective modes within microscopic models is very difficult because of their high excitation energies and different mechanisms contributing to the damping width. The so-called pygmy dipole resonance (PDR), a concentration of electric dipole strength below the well-known isovector electric giant dipole resonance (IVGDR), has attracted considerable interest during the past few years. In contrast to the IVGDR, the PDR is a low-lying mode located below the particle thresholds. Therefore, coupling to complex configurations is the only mechanism for the resonance damping. In addition, the density of complex configurations in the energy region of the PDR is not too high, allowing one to account for nearly all of them in a microscopic model. Therefore, the PDR is a challenge for theory in nuclear physics because one can expect a good description of the fragmentation of a collective mode without including any phenomenological parameters responsible for the resonance width. Thus, the comparison to experimental data makes it possible to determine whether the damping mechanism for a collective mode in many-body systems is well understood.

The first evidence for strong low-lying $E1$ excitations in heavy nuclei located in the energy region 5–10 MeV indicating an additional structure beside the IVGDR in the $E1$ response of atomic nuclei was found three decades ago [1–3]. Recently, an experimental survey of the whole mass region has revealed that the PDR is a common excitation mode in most atomic nuclei [4,5]. These experimental efforts are accompanied by intense theoretical investigations to find a microscopic description of the PDR and its properties; see, e.g., the review [6] and references therein. Understanding the nature of the low-lying $E1$ strength will, e.g., help to constrain the symmetry energy in atomic nuclei [7] and has an impact on reaction rates of astrophysical interest [8,9] as well as on the photodisintegration of ultrahigh-energy cosmic rays [10].

An ideal tool to study $E1$ strength below the neutron separation energy (S_n) is the method of real photon scattering or nuclear resonance fluorescence (NRF) [11,12]. With the advent of new powerful (γ, γ') setups, detailed information on the $E1$ strength distribution up to S_n of various medium-heavy and heavy nuclei could be obtained. The results of systematic surveys in the Ca isotopes [13], Ge isotopes [14], ^{88}Sr isotope [15], Sn isotopes [4,16], $N = 82$ isotones [17], and Pb isotopes [18,19] have shown a rather smooth variation of the position and total strength of the PDR. The availability of intense exotic beams allows one to extend the search for low-energy $E1$ strength to very neutron rich systems in Coulomb breakup experiments in inverse kinematics [20]. Using this method, neutron rich Sn and Sb isotopes have been studied at the FRS/LAND setup at GSI [21,22].

An enhancement of the integrated strength of the PDR to higher neutron-to-proton ratios N/Z is predicted in many microscopic model calculations [23–31]. The low-lying part of the $E1$ strength arises in most models from excess neutrons forming a neutron skin and oscillating against an isospin saturated core. It has been pointed out that in this case the total strength located in the PDR is connected to the thickness of the neutron skin and therefore might provide an alternative way to determine this nuclear parameter [7,29].

Up to now, mainly predictions of integral quantities such as total strengths and centroid energies have been compared to the experimental results. However, the experiments show a strong fragmentation of the observed $E1$ strength, which has two important consequences: First, the fragmentation will have an impact on integral quantities, as every experiment has a finite sensitivity limit, and second, the fragmentation itself provides another important quantity to compare theory and experiment, as already mentioned in the first paragraph. This Letter establishes for the first time a detailed look at the PDR fine structure and examines the corresponding calculations within the quasiparticle phonon model (QPM) [32]. In addition, the results of (γ, γ') experiments on ^{136}Xe finalizing

the systematics on the stable $N = 82$ isotones are presented.

The experiment was performed at the high intensity photon setup at the superconducting electron linear accelerator *S*-DALINAC at the Technische Universität Darmstadt [17]. Bremsstrahlung was produced by stopping the electron beam in a thick radiator. The high-pressure ^{136}Xe gas target (2.925 g) was sandwiched between two boron disks for photon flux calibrations. The scattered photons were detected by three large-volume high-purity germanium (HPGe) detectors, at 90° and 130° with respect to the incoming photon beam.

Figure 1 shows the measured photon spectrum of one of the detectors at 130° normalized to the product of the photon flux and the absolute photopeak efficiency of the detector. Therefore, the peak areas in this spectrum are directly proportional to the integrated cross sections of the corresponding transitions in the (γ, γ') reaction. The spectrum shows a concentration of strong peaks in the energy range between 5.5 and 7.5 MeV. In contrast, only a couple of small peaks are observed in the region just below the neutron separation energy S_n.

In NRF experiments, the experimental cross section for elastic scattering is proportional to Γ_0^2/Γ, with the decay width to the ground state Γ_0 and the total decay width Γ. In most cases, no inelastic transitions to excited states are observed, and $\Gamma_0/\Gamma = 1$ is assumed. However, one should keep in mind that weak unobserved branchings might result in a somewhat smaller ratio Γ_0/Γ, and therefore the extracted values for Γ_0 are only a lower limit.

From the angular distribution of the scattered photons, $J = 1$ can be assigned to all excited levels, while the parity was not accessible in this experiment. However, the parities of many bound $J = 1$ excitations have been measured in the neighboring isotones ^{138}Ba [33] and ^{140}Ce, and no positive parity state has been observed. Assuming negative parity for the observed states in ^{136}Xe is therefore well justified. For each state, the $B(E1)\uparrow$ strength can be calculated from the deduced Γ_0 values. The observed distribution as a function of excitation energy is presented in the upper part of Fig. 2 (the preliminary results published in Ref. [12] have to be rectified by the present values). The sensitivity limit of the experiment (indicated as a dotted line) is based on the background in the spectrum. This limit represents the minimum strength of a state that would result in a peak visible above the background with a confidence limit of at least 3σ.

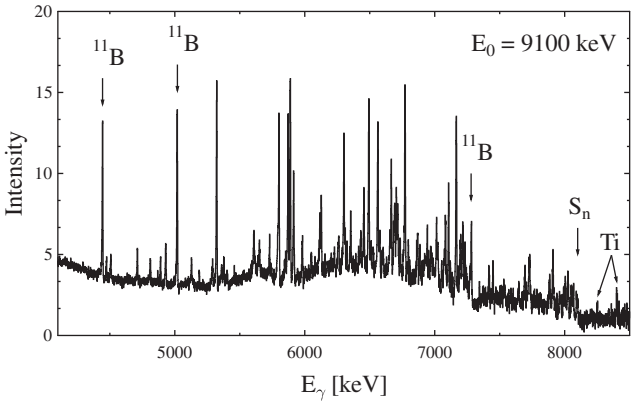

FIG. 1. Spectrum of one HPGe detector normalized to the incoming photon flux and the photopeak efficiency.

The $B(E1)\uparrow$ strength distribution in ^{136}Xe shows a concentration in the energy range between 5.5 and 7.5 MeV. A comparable resonancelike structure of $E1$ strength which is interpreted as the PDR is also observed in all other stable $N = 82$ isotones as reported in Ref. [17]. The measured integrated $B(E1)\uparrow$ strengths up to the neutron separation energy of the PDR in the stable $N = 82$ isotones are shown in Fig. 3. The new value for ^{136}Xe confirms the enhancement of the total observed strength for higher neutron-to-proton ratios N/Z, which is predicted by most microscopic model calculations. The prediction for ^{136}Xe presented in Ref. [17] is in excellent agreement with the measured value.

New calculations within the QPM have been performed. Excited states of nuclei are treated by this model in terms of quasiparticle random-phase approximation phonons which include both collective and almost pure 1p1h excitations. In the present calculation for ^{136}Xe, we have used the same set of model parameters as in the previous calculations for $N = 82$ isotones in Ref. [34]. Since the main goal of the calculation is to consider how well theory is able to describe the observed fragmentation of the $E1$ strength, the model space should be as large as possible. For this reason, the configuration space used in Ref. [34] has been extended by adding three-phonon (3ph) configu-

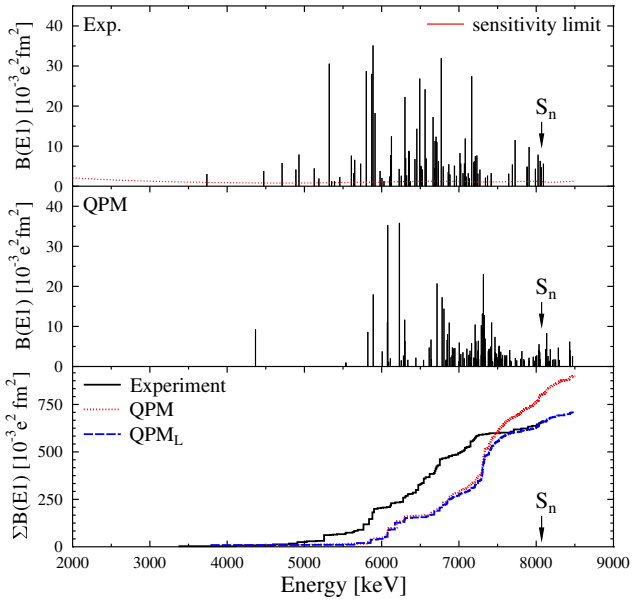

FIG. 2 (color online). Measured and calculated $B(E1)\uparrow$ strength distributions. For details, see the text.

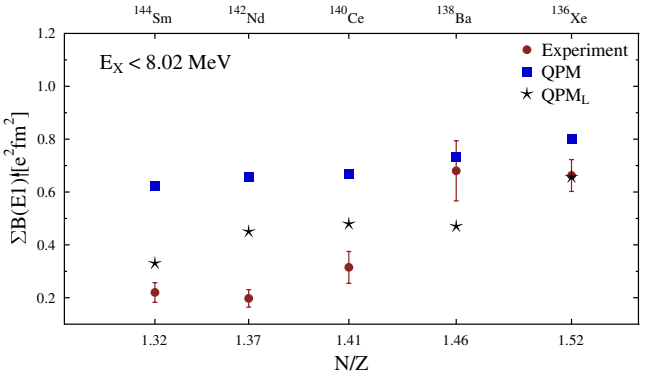

FIG. 3 (color online). Measured integrated $B(E1)\uparrow$ up to 8 MeV in the $N = 82$ isotones. The new value for ^{136}Xe confirms the enhancement for higher neutron-to-proton ratios N/Z.

rations; i.e., our wave function contains 1ph, 2ph, and 3ph components. It is essential that almost all $E1$ strength is carried by 1ph configurations while complex (2ph and 3ph) configurations participate in the fragmentation. Complex configurations are constructed from phonons of different multipolarities from $1^{\pm}$ to $9^{\pm}$ and with different internal fermionic structures. They have been truncated at 8.5 MeV, and Pauli principle corrections are neglected. Altogether, we have about 1150 configurations below 8.5 MeV and, accordingly, the same number of excited 1^- states after diagonalization of the model Hamiltonian. Keeping in mind that the lowest 4ph 1^- configuration in ^{136}Xe is expected at 7.2 MeV, our model space is almost complete below 8.5 MeV.

The results of the QPM calculation are shown in the middle part of Fig. 2. As in the experiment, a resonancelike structure of strongly fragmented $E1$ strength appears in the energy region between 6.0 and 8.0 MeV. The fact that the calculation also reproduces the fragmentation of the strength allows us to consider the finite experimental sensitivity in the comparison to the data and, furthermore, to compare not only integral quantities but also the fragmentation itself.

In the lower part of Fig. 2, the running sum of the $E1$ strength is given for the experiment and calculation. For the calculation, two running sums are presented, one including all states (QPM) and one including only states with strengths above the sensitivity limit of the experiment (QPM_L). Besides a shift of about 500 keV to higher energies, the shapes of the QPM_L sum and the experimental data are in excellent agreement. The exclusion of states below the sensitivity limit of the experiment changes the QPM sum only in the energy region above 7.5 MeV. Up to the neutron separation energy, the integrated strengths for the QPM and the QPM_L sum are 0.802 and $0.655e^2$ fm^2, respectively. On the one hand, the latter value agrees very well with the experimental result of $0.662(45)e^2$ fm^2, and, on the other hand, it shows that only a smaller fraction of the total strength is carried by weak excitations up to S_n.

The calculated values of the total $B(E1)\uparrow$ strength within the QPM up to 8.02 MeV (S_n of ^{136}Xe) for all stable $N = 82$ isotones are shown in Fig. 3 together with the experimental results. By accounting for the sensitivity limit of the corresponding (γ, γ') experiments in the QPM sum (QPM_L), the overall agreement is clearly improved.

To compare the spreading of the $E1$ strength in ^{136}Xe in the experiment and the QPM calculation, we determine the first moment σ of the $E1$ strength distribution:

$$\sigma = \sum_i |E_i - E_c| \frac{B(E1)_i}{\sum B(E1)}.$$

For the experimental data, we obtain $\sigma_{\mathrm{exp}} = 0.61(2)$ MeV and for the full QPM calculations $\sigma_{\mathrm{QPM}} = 0.53$ MeV. Accounting for the experimental sensitivity limit only slightly changes the value to $\sigma_{\mathrm{QPM}_L} = 0.52$ MeV. Thus, experiment and theory are in good agreement.

A comparison of the experimental data and the QPM calculation in light of the distribution and fragmentation of the observed $B(E1)$ strength is shown in Fig. 4. To focus on the distribution, the states are grouped in energy bins 250 keV wide on the left-hand side, while the right-hand side focuses on the fragmentation by grouping the states in bins of $1 \times 10^{-3} e^2$ fm^2. The upper row shows the corresponding number of states in the experiment and for the QPM calculation taking the experimental limit into account. The lower row compares the experimental data of the summed $B(E1)$ strength per bin to the QPM calculation and puts the focus on the effect of the experimental sensitivity limit for the calculation.

Experiment and calculation agree nicely for energies below about 7 MeV, where the included model space can be expected to be complete as explained above. Going to higher energies, the number of levels as well as the summed $B(E1)$ strength observed in the experiment are significantly lower than the calculated one even when

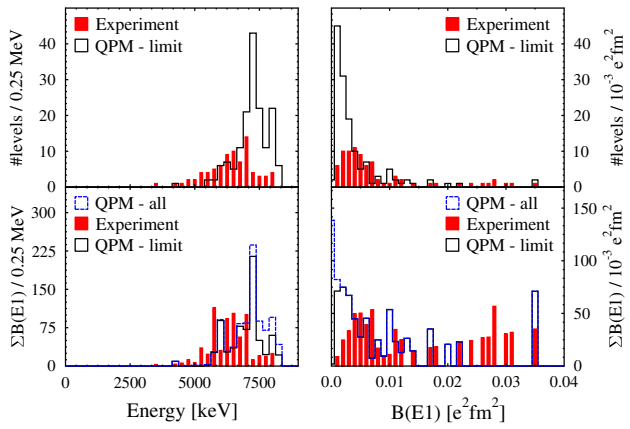

FIG. 4 (color online). Comparison of the experimentally observed and in the QPM calculation predicted $E1$ strength with respect to its distribution (left) and fragmentation (right). For details, see the text.

taking the sensitivity limit into account. However, the pattern of the summed $B(E1)$ strength distribution basically does not change by accounting for the sensitivity limit in the QPM as can be seen in the lower-left part of Fig. 4. Compared to the lower part of Fig. 2, it becomes clear that these experimentally missing states do not carry much strength as is mirrored in the right part of Fig. 4. Here experiment and calculation agree well for excitations with a value of $B(E1) \geq 3 \times 10^{-3} e^2$ fm^2 taking into account the absolute value as well as the shape of both distributions.

Discrepancies occur for excitations with lower $B(E1)$ values. Both observations are based on the same reasons: First, at excitation energies above 7 MeV, the model space in the QPM calculation is not complete any more due to the occurrence of 4ph configurations. Thus, the calculation might underestimate the fragmentation which would cause the strength to split into more states with weaker strengths so that the states are no longer observable within the experimental sensitivity limit. Second, the experimental limit as defined here cannot be expected to be a rigid limit. As mentioned above, the limit is given by the minimum strength for an excitation to result in a peak above the background observed in the spectrum. However, if many weak unresolved excitations contribute to the continuous part of the spectrum, this limit no longer represents an absolute detection limit but provides the amount of strength an excitation has to exceed the surrounding sea of weak excitations. Consequently, the number of experimentally detected states decreases for $B(E1) \leq 3 \times 10^{-3} e^2$ fm^2 although one expects the increasing behavior as seen in the QPM calculations, thus reflecting the limits of the experimental method. However, the selectivity of the method to the $B(E1)$ strength ensures the observation of all states above $B(E1) = 3 \times 10^{-3} e^2$ fm^2. Hence, the overall agreement of experimental data and QPM calculations is very good because the resonancelike structure of the $E1$ strength as well as the amount of fragmentation is reproduced in the constraints of the limits of the experimental method and the model space in use.

In conclusion, the photoresponse of the semimagic $N = 82$ isotone ^{136}Xe measured in real photon scattering shows a resonancelike concentration well below the neutron separation energy. The total amount, the distribution, and the fragmentation of the strength is well reproduced in QPM calculations. This confirms that the damping mechanism of the PDR is the coupling of a collective mode with complex configurations. The results show that the fragmentation provides a deeper test of modern microscopic model calculations.

However, further observables of the models should be measured to learn more about the underlying structure of the $E1$ strength. Recent experiments on ^{140}Ce using the $(\alpha, \alpha', \gamma)$ reaction have revealed a splitting of the PDR into two parts [35], which points to different structures within the PDR. The comparison to such data obtained in hadron-scattering experiments will help to further constrain microscopic models.

The authors acknowledge the help of M. Babilon, M. Elvers, J. Endres, B. Özel, L. Schnorrenberger, and S. Volz during the experiment. We further thank U. Kneissl, M. Krticka, P. von Neumann-Cosel, N. Pietralla, A. Richter, and H. Wörtche for stimulating discussions. This work was supported by the Deutsche Forschungsgemeinschaft (Contract No. SFB 634).

*savran@ikp.tu-darmstadt.de
†Permanent address: JINR, Dubna, Russia.

[1] G. A. Bartholomew *et al.*, Adv. Nucl. Phys. **7**, 229 (1973).
[2] F. R. Metzger, Phys. Rev. C **18**, 1603 (1978).
[3] F. R. Metzger, Phys. Rev. C **18**, 2138 (1978).
[4] K. Govaert *et al.*, Phys. Rev. C **57**, 2229 (1998).
[5] A. Zilges *et al.*, Phys. Lett. B **542**, 43 (2002).
[6] N. Paar *et al.*, Rep. Prog. Phys. **70**, 691 (2007).
[7] J. Piekarewicz, Phys. Rev. C **73**, 044325 (2006).
[8] S. Goriely, Phys. Lett. B **436**, 10 (1998).
[9] S. Goriely *et al.*, Nucl. Phys. **A739**, 331 (2004).
[10] E. Khan *et al.*, Astropart. Phys. **23**, 191 (2005).
[11] U. Kneissl *et al.*, Prog. Part. Nucl. Phys. **37**, 349 (1996).
[12] U. Kneissl *et al.*, J. Phys. G **32**, R217 (2006).
[13] T. Hartmann *et al.*, Phys. Rev. Lett. **93**, 192501 (2004).
[14] A. Jung *et al.*, Nucl. Phys. **A584**, 103 (1995).
[15] R. Schwengner *et al.*, Phys. Rev. C **76**, 034321 (2007).
[16] B. Ozel *et al.*, Nucl. Phys. **A788**, 385 (2007).
[17] S. Volz *et al.*, Nucl. Phys. **A779**, 1 (2006).
[18] N. Ryezayeva *et al.*, Phys. Rev. Lett. **89**, 272502 (2002).
[19] J. Enders *et al.*, Nucl. Phys. **A724**, 243 (2003).
[20] T. Aumann, Eur. Phys. J. A **26**, 441 (2005).
[21] P. Adrich *et al.*, Phys. Rev. Lett. **95**, 132501 (2005).
[22] A. Klimkiewicz *et al.*, Nucl. Phys. **A788**, 145 (2007).
[23] G. Tertychny *et al.*, Phys. Lett. B **647**, 104 (2007).
[24] J. Terasaki *et al.*, Phys. Rev. C **76**, 044320 (2007).
[25] J. Liang *et al.*, Phys. Rev. C **75**, 054320 (2007).
[26] V. Tselyaev *et al.*, Phys. Rev. C **75**, 014315 (2007).
[27] J. Terasaki *et al.*, Phys. Rev. C **74**, 044301 (2006).
[28] N. Paar *et al.*, Phys. Lett. B **606**, 288 (2005).
[29] N. Tsoneva *et al.*, Phys. Lett. B **586**, 213 (2004).
[30] G. Colò *et al.*, Phys. Lett. B **485**, 362 (2000).
[31] D. Sarchi *et al.*, Phys. Lett. B **601**, 27 (2004).
[32] V. G. Soloviev, *Theory of Atomic Nuclei: Quasiparticles and Phonons* (Institute of Physics, Bristol, 1992).
[33] N. Pietralla *et al.*, Phys. Rev. Lett. **88**, 012502 (2001).
[34] J. Enders *et al.*, Nucl. Phys. **A741**, 3 (2004).
[35] D. Savran *et al.*, Phys. Rev. Lett. **97**, 172502 (2006).